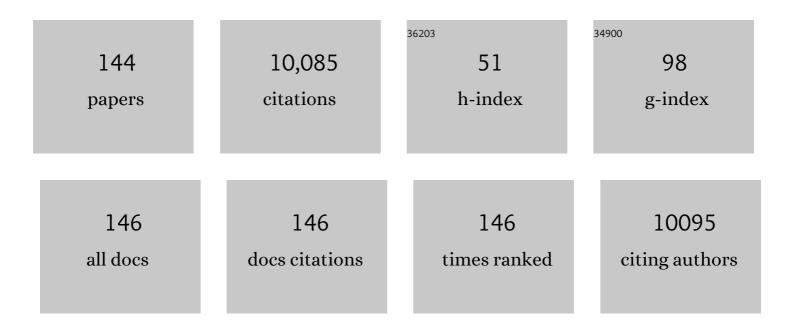
Kevin F Mccarty

List of Publications by Year in descending order

Source: https://exaly.com/author-pdf/6511513/publications.pdf Version: 2024-02-01



#	Article	IF	CITATIONS
1	The Role of Surface Oxygen in the Growth of Large Single-Crystal Graphene on Copper. Science, 2013, 342, 720-723.	6.0	977
2	Review of advances in cubic boron nitride film synthesis. Materials Science and Engineering Reports, 1997, 21, 47-100.	14.8	567
3	Heteroepitaxial Growth of Two-Dimensional Hexagonal Boron Nitride Templated by Graphene Edges. Science, 2014, 343, 163-167.	6.0	479
4	Graphene Islands on Cu Foils: The Interplay between Shape, Orientation, and Defects. Nano Letters, 2010, 10, 4890-4896.	4.5	337
5	Evidence for graphene growth by C cluster attachment. New Journal of Physics, 2008, 10, 093026.	1.2	262
6	Measuring fundamental properties in operating solid oxide electrochemical cells by using in situ X-ray photoelectron spectroscopy. Nature Materials, 2010, 9, 944-949.	13.3	257
7	Factors influencing graphene growth on metal surfaces. New Journal of Physics, 2009, 11, 063046.	1.2	241
8	Ionâ€assisted pulsed laser deposition of cubic boron nitride films. Journal of Applied Physics, 1994, 76, 3088-3101.	1.1	235
9	Intercalation Pathway in Many-Particle LiFePO ₄ Electrode Revealed by Nanoscale State-of-Charge Mapping. Nano Letters, 2013, 13, 866-872.	4.5	206
10	On the role of ions in the formation of cubic boron nitride films by ion-assisted deposition. Journal of Materials Research, 1994, 9, 2925-2938.	1.2	201
11	Origin of the mosaicity in graphene grown on Cu(111). Physical Review B, 2011, 84, .	1.1	183
12	Defects of graphene on Ir(111): Rotational domains and ridges. Physical Review B, 2009, 80, .	1.1	181
13	A Raman study of the systems Fe3â^'xCrxO4 and Fe2â^'xCrxO3. Journal of Solid State Chemistry, 1989, 79, 19-27.	1.4	177
14	Highly Enhanced Concentration and Stability of Reactive Ce ³⁺ on Doped CeO ₂ Surface Revealed In Operando. Chemistry of Materials, 2012, 24, 1876-1882.	3.2	169
15	Growth from below: bilayer graphene on copper by chemical vapor deposition. New Journal of Physics, 2012, 14, 093028.	1.2	150
16	Electronic structure of graphene on single-crystal copper substrates. Physical Review B, 2011, 84, .	1.1	148
17	In-plane orientation effects on the electronic structure, stability, and Raman scattering of monolayer graphene on Ir(111). Physical Review B, 2011, 83, .	1.1	146
18	The relationship between the spatially resolved field emission characteristics and the raman spectra of a nanocrystalline diamond cold cathode. Applied Physics Letters, 1996, 69, 3842-3844.	1.5	144

Kevin F Mccarty

#	Article	IF	CITATIONS
19	Raman-active phonons of a twin-freeYBa2Cu3O7crystal: A complete polarization analysis. Physical Review B, 1990, 41, 8792-8797.	1.1	140
20	Inelastic light scattering in α-Fe2O3: Phonon vs magnon scattering. Solid State Communications, 1988, 68, 799-802.	0.9	131
21	Thermal stability of amorphous carbon films grown by pulsed laser deposition. Applied Physics Letters, 1996, 68, 1643-1645.	1.5	122
22	Orientation-dependent work function of graphene on Pd(111). Applied Physics Letters, 2010, 97, .	1.5	122
23	Structure of theαâ^'Al2O3(0001)surface from low-energy electron diffraction: Al termination and evidence for anomalously large thermal vibrations. Physical Review B, 2002, 65, .	1.1	115
24	Oxidation of Graphene on Metals. Journal of Physical Chemistry C, 2010, 114, 5134-5140.	1.5	111
25	Vacancies in solids and the stability of surface morphology. Nature, 2001, 412, 622-625.	13.7	107
26	Growth from Below: Graphene Bilayers on Ir(111). ACS Nano, 2011, 5, 2298-2306.	7.3	105
27	Kinetics and thermodynamics of carbon segregation and graphene growth on Ru(0001). Carbon, 2009, 47, 1806-1813.	5.4	104
28	Microstructure of cubic boron nitride thin films grown by ionâ€assisted pulsed laser deposition. Journal of Applied Physics, 1994, 76, 295-303.	1.1	102
29	Self-limiting growth of copper islands on TiO2(110)-(1×1). Surface Science, 2000, 450, 78-97.	0.8	98
30	The synthesis, characterization, and mechanical properties of thick, ultrahard cubic boron nitride films deposited by ion-assisted sputtering. Journal of Applied Physics, 1997, 82, 1617-1625.	1.1	97
31	Scanning tunneling microscopy study of graphene on Au(111): Growth mechanisms and substrate interactions. Physical Review B, 2012, 85, .	1.1	89
32	The surface structure of α-Al2O3 determined by low-energy electron diffraction: aluminum termination and evidence for anomolously large thermal vibrations. Surface Science, 2000, 464, L732-L738.	0.8	81
33	In Situ Characterization of Ceria Oxidation States in High-Temperature Electrochemical Cells with Ambient Pressure XPS. Journal of Physical Chemistry C, 2010, 114, 19853-19861.	1.5	81
34	Graphene growth on metal surfaces. MRS Bulletin, 2012, 37, 1158-1165.	1.7	81
35	Surface and interface segregation in β-NiAl with and without Pt addition. Scripta Materialia, 2006, 54, 937-941.	2.6	79
36	Extraordinary epitaxial alignment of graphene islands on Au(111). New Journal of Physics, 2012, 14, 053008.	1.2	78

#	Article	IF	CITATIONS
37	Growth of cubic BN films on βâ€SiC by ionâ€assisted pulsed laser deposition. Applied Physics Letters, 1995, 66, 2813-2815.	1.5	77
38	Orientation relationships in heteroepitaxial aluminum films on sapphire. Thin Solid Films, 1997, 299, 110-114.	0.8	73
39	Lattice dynamics ofNaAlH4from high-temperature single-crystal Raman scattering andab initiocalculations:â€∫Evidence of highly stableAlH4â^anions. Physical Review B, 2005, 71, .	1.1	71
40	Magnetism in nanometer-thick magnetite. Physical Review B, 2012, 85, .	1.1	71
41	Small, uniform, and thermally stable silver particles on TiO2(110)-(1×1). Surface Science, 2000, 464, L708-L714.	0.8	68
42	Imaging Spin-Reorientation Transitions in Consecutive Atomic Co Layers on Ru(0001). Physical Review Letters, 2006, 96, 147202.	2.9	68
43	Preparation and Raman analysis of single-phaseY1â^xPrxBa2Cu3O7â^1^. Physical Review B, 1989, 39, 12383-12386.	1.1	67
44	Unusual role of epilayer–substrate interactions in determining orientational relations in van der Waals epitaxy. Proceedings of the National Academy of Sciences of the United States of America, 2014, 111, 16670-16675.	3.3	64
45	Hydrodesulfurization catalysis by Chevrel phase compounds. Journal of Catalysis, 1985, 93, 375-387.	3.1	63
46	Analysis of residual stress in cubic boron nitride thin films using micromachined cantilever beams. Diamond and Related Materials, 1996, 5, 1295-1302.	1.8	62
47	Effects of ambient conditions on the adhesion of cubic boron nitride films on silicon substrates. Thin Solid Films, 1994, 253, 130-135.	0.8	61
48	Herringbone and triangular patterns of dislocations in Ag, Au, and AgAu alloy films on Ru(0001). Surface Science, 2006, 600, 1735-1757.	0.8	60
49	High-temperature Raman measurements of single-crystalYBa2Cu3O7â^'x. Physical Review B, 1988, 38, 2914-2917.	1.1	59
50	Crystallographic texture in cubic boron nitride thin films. Journal of Applied Physics, 1996, 79, 3567-3571.	1.1	56
51	Enhanced Self-Diffusion on Cu(111) by Trace Amounts of S: Chemical-Reaction-Limited Kinetics. Physical Review Letters, 2004, 93, 166101.	2.9	54
52	Insight into Magnetite's Redox Catalysis from Observing Surface Morphology during Oxidation. Journal of the American Chemical Society, 2013, 135, 10091-10098.	6.6	53
53	Temperature dependence of the linewidths of the Raman-active phonons ofYBa2Cu3O7: Evidence for a superconducting gap between 440 and 500cmâ^1. Physical Review B, 1991, 43, 13751-13754.	1.1	52
54	Pulsed laser deposition of BN onto silicon (100) substrates at 600 °C. Thin Solid Films, 1994, 237, 48-56.	0.8	52

#	Article	IF	CITATIONS
55	Graphene growth by metal etching on Ru(0001). Physical Review B, 2009, 80, .	1.1	51
56	Raman analysis of TlCa2Ba2Cu3O19 and Tl2Ca2Ba2Cu3O10 crystals. Physica C: Superconductivity and Its Applications, 1989, 157, 135-143.	0.6	50
57	Determining the structure of Ru(0001) from low-energy electron diffraction of a single terrace. Surface Science, 2006, 600, L105-L109.	0.8	50
58	Electron-phonon coupling in superconductingBa0.6K0.4BiO3: A Raman scattering study. Physical Review B, 1989, 40, 2662-2665.	1.1	49
59	Electronic Raman scattering ofYBa2Cu3O7usingc-axis polarization: Evidence for two characteristic superconducting energies. Physical Review B, 1990, 42, 9973-9977.	1.1	49
60	Substrate effects in cubic boron nitride film formation. Journal of Vacuum Science and Technology A: Vacuum, Surfaces and Films, 1996, 14, 251-255.	0.9	49
61	Deuterodesulfurization of thiophene: An investigation of the reaction mechanism. Journal of Catalysis, 1987, 103, 261-269.	3.1	48
62	Measuring individual overpotentials in an operating solid-oxide electrochemical cell. Physical Chemistry Chemical Physics, 2010, 12, 12138.	1.3	48
63	Oxidation stages of Ni electrodes in solid oxide fuel cell environments. Physical Chemistry Chemical Physics, 2013, 15, 8334.	1.3	47
64	Evidence for rhombohedral boron nitride in cubic boron nitride films grown by ion-assisted deposition. Physical Review B, 1994, 50, 7884-7887.	1.1	46
65	Role of Bulk Thermal Defects in the Reconstruction Dynamics of theTiO2(110)Surface. Physical Review Letters, 2003, 90, 046104.	2.9	46
66	Resonance Raman spectroscopy of G-line and folded phonons in twisted bilayer graphene with large rotation angles. Applied Physics Letters, 2013, 103, .	1.5	46
67	Crucial role of substrate steps in de-wetting of crystalline thin films. Surface Science, 2004, 570, L297-L303.	0.8	45
68	Oxidation Pathways in Bicomponent Ultrathin Iron Oxide Films. Journal of Physical Chemistry C, 2012, 116, 11539-11547.	1.5	44
69	Anharmonic effects and the two-particle continuum in the Raman spectra ofYBa2Cu3O6.9,TlBa2CaCu2O7, andTl2Ba2CaCu2O8. Physical Review B, 1993, 47, 8910-8916.	1.1	42
70	Structure and morphology of ultrathinCo/Ru(0001) films. New Journal of Physics, 2007, 9, 80-80.	1.2	40
71	Note: Fixture for characterizing electrochemical devices in-operando in traditional vacuum systems. Review of Scientific Instruments, 2010, 81, 086104.	0.6	39
72	Cubic boron nitride formation on Si (100) substrates at room temperature by pulsed laser deposition. Applied Physics Letters, 1992, 61, 2406-2408.	1.5	38

#	Article	IF	CITATIONS
73	Hydrodesulfurization by reduced molybdenum sulfides: activity and selectivity of Chevrel phase catalysts. Industrial & Engineering Chemistry Product Research and Development, 1984, 23, 519-524.	0.5	37
74	On the initial stages of AlN thin-film growth onto (0001) oriented Al2O3 substrates by molecular beam epitaxy. Journal of Applied Physics, 1999, 85, 466-472.	1.1	37
75	Growth structure and work function of bilayer graphene on Pd(111). Physical Review B, 2012, 85, .	1.1	37
76	Room temperature in-plane âŸ 100⟩ magnetic easy axis for Fe3O4/SrTiO3(001):Nb grown by infrared pulsed laser deposition. Journal of Applied Physics, 2013, 114, .	1.1	37
77	Noble metal capping effects on the spin-reorientation transitions of Co/Ru(0001). New Journal of Physics, 2008, 10, 073024.	1.2	34
78	Diffusion mechanisms in chemical vapor-deposited iridium coated on chemical vapor-deposited rhenium. Metallurgical and Materials Transactions A - Physical Metallurgy and Materials Science, 1992, 23, 851-855.	1.4	33
79	Orientation-dependence of elastic strain energy in hexagonal and cubic boron nitride layers in energetically deposited BN films. Journal of Vacuum Science and Technology A: Vacuum, Surfaces and Films, 1997, 15, 196-200.	0.9	33
80	Growth regimes of the oxygen-deficient TiO2(110) surface exposed to oxygen. Surface Science, 2003, 543, 185-206.	0.8	33
81	Real-time observation of epitaxial graphene domain reorientation. Nature Communications, 2015, 6, 6880.	5.8	33
82	Metallization and superconducting properties ofYBa2Cu3O6.2Bry. Physical Review B, 1990, 41, 11140-11148.	1.1	32
83	Lowâ€ŧemperature diamond growth in a microwave discharge. Applied Physics Letters, 1989, 55, 2739-2741.	1.5	31
84	Scaleable stagnationâ€flow reactors for uniform materials deposition: Application to combustion synthesis of diamond. Applied Physics Letters, 1993, 63, 1498-1500.	1.5	29
85	The 1×1/1×2 phase transition of the TiO2() surface––variation of transition temperature with crystal composition. Surface Science, 2003, 527, L203-L212.	0.8	29
86	Structure and magnetism in ultrathin iron oxides characterized by low energy electron microscopy. Journal of Physics Condensed Matter, 2009, 21, 314011.	0.7	29
87	How metal films de-wet substrates—identifying the kinetic pathways and energetic driving forces. New Journal of Physics, 2009, 11, 043001.	1.2	29
88	Electron reflectivity measurements of Ag adatom concentrations on W(110). Surface Science, 2006, 600, 4062-4066.	0.8	27
89	Raman analysis of single-crystal, lead-doped TlCaBa2Cu2O7. Physica C: Superconductivity and Its Applications, 1988, 156, 119-125.	0.6	25
90	SuperconductingLa2CuO4+xprepared by oxygenation at high pressure: A Raman-scattering study. Physical Review B, 1991, 43, 7883-7890.	1.1	24

Kevin F Mccarty

#	Article	IF	CITATIONS
91	On the low-temperature threshold for cubic boron nitride formation in energetic film deposition. Diamond and Related Materials, 1996, 5, 1519-1526.	1.8	24
92	Structure and magnetism of ultra-thin chromium layers on W(110). New Journal of Physics, 2008, 10, 013005.	1.2	24
93	Raman microprobe analysis of Tl-Ca-Ba-Cu-O polycrystals. Solid State Communications, 1988, 68, 77-80.	0.9	23
94	Spatially resolved dynamics of the TiO2(110) surface reconstruction. Surface Science, 2003, 540, 157-171.	0.8	23
95	Self-assembly and dynamics of oxide nanorods on NiAl(110). Physical Review B, 2005, 71, .	1.1	23
96	Stability of ultrathin alumina layers on NiAl(110). Physical Review B, 2008, 77, .	1.1	21
97	Viable thermionic emission from graphene-covered metals. Applied Physics Letters, 2012, 100, 181604.	1.5	21
98	Comparison of the Raman-active phonons of YBa2Cu3O7 crystals grown in gold and zirconia crucibles. Physica C: Superconductivity and Its Applications, 1992, 192, 331-350.	0.6	20
99	The Importance of Threading Dislocations on the Motion of Domain Boundaries in Thin Films. Science, 2005, 308, 1303-1305.	6.0	20
100	How plastic deformation can produce texture in graphitic films of boron nitride, carbon nitride, and carbon. Diamond and Related Materials, 1997, 6, 1219-1225.	1.8	19
101	InsituRaman spectroscopy of diamond during growth in a hot filament reactor. Journal of Applied Physics, 1992, 72, 2001-2005.	1.1	18
102	Translation-related domain boundaries form to relieve strain in a thin alumina film on NiAl (110). Applied Physics Letters, 2006, 88, 141902. Nanoscale Periodicity in String-Forming, Systems at High Temperature combination.	1.5	18
103	xmlns:mml="http://www.w3.org/1998/Math/MathML" display="inline"> <mml:mi>Au</mml:mi> <mml:mo>/</mml:mo> <mml:mi mathvariant="normal">W<mml:mo stretchy="false">(<mml:mn>110</mml:mn><mml:mo) 0.784314="" 1="" 10="" 50<="" etoo1="" overlock="" rgbt="" td="" tf="" ti=""><td>2.9 0 242 Td (</td><td>18 stretchv="fa</td></mml:mo)></mml:mo </mml:mi 	2.9 0 242 Td (18 stretchv="fa
104	Work function of a quasicrystal surface: Icosahedral Al–Pd–Mn. Journal of Vacuum Science and Technology A: Vacuum, Surfaces and Films, 2009, 27, 1249-1250.	0.9	18
105	Diamond deposition on polycrystalline films of cubic boron nitride. Applied Physics Letters, 1993, 63, 1342-1344.	1.5	16
106	Largeâ€area diamond deposition in an atmospheric pressure stagnationâ€flow reactor. Applied Physics Letters, 1996, 68, 2158-2160.	1.5	16
107	Imaging the crystallization and growth of oxide domains on the NiAl(110) surface. Surface Science, 2001, 474, L165-L172.	0.8	16
108	Twin Boundaries Can Be Moved by Step Edges During Film Growth. Physical Review Letters, 2005, 95, 166105.	2.9	16

#	Article	IF	CITATIONS
109	CO-Assisted Subsurface Hydrogen Trapping in Pd(111) Films. Journal of Physical Chemistry Letters, 2012, 3, 87-91.	2.1	16
110	Site-selective oxygen-isotope substitution inYBa2Cu3O7â~'δ. Physical Review B, 1991, 44, 9556-9561.	1.1	15
111	Determination of diamond film quality during growth using in situ Raman spectroscopy. Diamond and Related Materials, 1994, 3, 22-29.	1.8	15
112	Three-fold diffraction symmetry in epitaxial graphene and the SiC substrate. Physical Review B, 2009, 80, .	1.1	15
113	Structure of ultrathin Pd films determined by low-energy electron microscopy and diffraction. New Journal of Physics, 2010, 12, 023023.	1.2	15
114	Electrochemical intermediate species and reaction pathway in H2 oxidation on solid electrolytes. Chemical Communications, 2012, 48, 8338.	2.2	15
115	Deposition and analysis of Ir-Al coatings for oxidation protection of carbon materials at high temperatures. Surface and Coatings Technology, 1990, 42, 29-40.	2.2	14
116	Surface dynamics dominated by bulk thermal defects: The case ofNiAl(110). Physical Review B, 2005, 71, .	1.1	14
117	Hydrogen-induced reversible spin-reorientation transition and magnetic stripe domain phase in bilayer Co on Ru(0001). Physical Review B, 2012, 85, .	1.1	14
118	Raman scattering as a technique of measuring film thickness: interference effects in thin growing films. Applied Optics, 1987, 26, 4482.	2.1	12
119	Deterministic Positioning of Three-Dimensional Structures on a Substrate by Film Growth. Nano Letters, 2006, 6, 858-861.	4.5	12
120	Determination of the surface structure of CeO2(111) by low-energy electron diffraction. Journal of Chemical Physics, 2013, 139, 114703.	1.2	12
121	Effect of gold-doping on the energy gap of YBa2Cu3O7 as determined by Raman scattering. Solid State Communications, 1991, 79, 359-362.	0.9	11
122	Micromachined silicon cantilever beams for thin-film stress measurement. Thin Solid Films, 1996, 287, 214-219.	0.8	11
123	Preferred orientation in carbon and boron nitride: Does a thermodynamic theory of elastic strain energy get it right?. Journal of Vacuum Science and Technology A: Vacuum, Surfaces and Films, 1999, 17, 2749-2752.	0.9	11
124	Influence of lattice orientation on growth and structure of graphene on Cu(0 0 1). Carbon, 2015, 90, 284-290.	5.4	11
125	Crystal growth rate limited by step length — the case of oxygen-deficient TiO2 exposed to oxygen. Journal of Crystal Growth, 2004, 270, 691-698.	0.7	10
126	Evolution of a Reactive Surface via Subsurface Defect Dynamics. Physical Review Letters, 2007, 99, 026101.	2.9	9

#	Article	IF	CITATIONS
127	Temperature dependence of the phonon frequencies, linewidths, and Raman-continuum scattering of single-domainY0.56Pr0.44Ba2Cu3O7. Physical Review B, 1992, 46, 11958-11964.	1.1	8
128	Real-space study of the growth of magnesium on ruthenium. Surface Science, 2011, 605, 903-911.	0.8	8
129	Comment on â€~â€~Growth and characterization of epitaxial cubic boron nitride films on silicon''. Physical Review B, 1994, 50, 8907-8910.	1.1	7
130	Real-Time Measurements of Deposit Formation from Sodium Sulfate-Seeded Flames. Combustion Science and Technology, 1987, 54, 51-60.	1.2	6
131	Dependence of the excitation wavelength on the Raman-active phonons of YBa2Cu3O7. Physica C: Superconductivity and Its Applications, 1992, 200, 315-322.	0.6	6
132	Real Space Observations of Magnesium Hydride Formation and Decomposition. Chemistry of Materials, 2010, 22, 1291-1293.	3.2	5
133	Low-Energy Electron Microscopy. Springer Series in Surface Sciences, 2013, , 531-561.	0.3	5
134	In Situ Raman Spectroscopy of High Temperature Pyrite Reactions Related to Deposit Formation from Coal. Journal of the Electrochemical Society, 1989, 136, 1223-1229.	1.3	4
135	Preparation of wurtzitic AlN thin films with a novel crystallographic alignment on MgO substrates by molecular-beam epitaxy. Journal of Materials Research, 1998, 13, 1414-1417.	1.2	4
136	Measuring the magnetization of three monolayer thick Co islands and films by x-ray dichroism. Physical Review B, 2009, 80, .	1.1	4
137	Valence band circular dichroism in non-magnetic Ag/Ru(0001) at normal emission. Journal of Physics Condensed Matter, 2011, 23, 305006.	0.7	4
138	Periodic step arrays on the aperiodic <mml:math <br="" xmlns:mml="http://www.w3.org/1998/Math/MathML">display="inline"><mml:mi>i</mml:mi></mml:math> -Al-Pd-Mn quasicrystal surface at high temperature. Physical Review B, 2010, 81, .	1.1	3
139	Observation of magnetic excitations in antiferromagnetic TlYBa2Cu2O7 by inelastic light scattering. Physica C: Superconductivity and Its Applications, 1989, 159, 603-608.	0.6	2
140	Systematic study of diamond film deposition in an atmospheric-pressure stagnation-flow flame reactor. Diamond and Related Materials, 1998, 7, 1320-1327.	1.8	1
141	<title>Superconducting La2CuO4+x prepared by oxygenation at high pressure: a Raman-scattering study</title> . , 1990, 1336, 77.		0
142	Pulsed Excimer Laser Ablation Deposition of Boron Nitride on Si (100) Substrates. Materials Research Society Symposia Proceedings, 1992, 242, 593.	0.1	0
143	Pulsed Microwave Processing of High-TC Superconducting Films. Materials Research Society Symposia Proceedings, 1992, 269, 187.	0.1	0
144	Electron Microscopy Study of Cubic Boron Nitride Thin Films Grown by Ion -Assisted Pulsed Laser Deposition. Materials Research Society Symposia Proceedings, 1993, 311, 373.	0.1	0